Physica E 83 (2016) 455–460

Contents lists available at ScienceDirect

Physica E

journal homepage: www.elsevier.com/locate/physe

Analytical insight into the lattice thermal conductivity and heat capacity of monolayer MoS_2

Dipankar Saha *, Santanu Mahapatra

Nano-Scale Device Research Laboratory, Department of Electronic Systems Engineering, Indian Institute of Science, Bangalore 560012, India

HIGHLIGHTS

- Semi-analytic solution of lattice thermal conductivity of the monolayer MoS_2 is proposed.
- The in-plane and the out-of-plane acoustic modes are considered.
- Closed-form expressions of the mode specific heat capacities have been formulated.
- Effective scattering includes the phonon-boundary scattering, along with the intrinsic one.
- The model could be useful to look into the electro-thermal behaviour of two dimensional TMDs.

ARTICLE INFO

Article history:
Received 23 November 2015
Received in revised form
11 January 2016
Accepted 13 January 2016
Available online 11 February 2016

Keywords:
Two dimensional transition-metal dichalcogenides
Monolayer MoS_2
Lattice thermal conductivity
First-principles calculations
Acoustic phonon

ABSTRACT

We report, a detailed theoretical study on the lattice thermal conductivity of a suspended monolayer MoS_2, far beyond its ballistic limit. The analytical approach adopted in this work mainly relies on the use of Boltzmann transport equation (BTE) within the relaxation time approximation (RTA), along with the first-principles calculations. Considering the relative contributions from the various in-plane and out-of-plane acoustic modes, we derive the closed-form expressions of the mode specific heat capacities, which we later use to obtain the phonon thermal conductivities of the monolayer MoS_2. Besides finding the intrinsic thermal conductivity, we also analyse the effect of the phonon-boundary scattering, for different dimensions and edge roughness conditions. The viability of the semi-analytic solution of lattice thermal conductivity reported in this work ranges from a low temperature (T~30 K) to a significantly high temperature (T~550 K), and the room temperature (RT) thermal conductivity value has been obtained as 34.06 W m^{-1} K^{-1} which is in good agreement with the experimental result.

1. Introduction

Molybdenite (MoS_2) which belongs to the family of two dimensional (2D) transition-metal dichalcogenides (TMDs) has gained a significant research interest in the past few years, specially due to its inherent finite bandgap value [1–3]. MoS_2, which is generally semiconducting in nature, shows a direct bandgap of 1.8 eV for monolayer [1,4]. Thus, it can effectively be used as the alternative channel material in FET devices [1,5]. Besides, owing to its distinct properties like broken inversion symmetry leading to spin–orbit coupling [6], higher mechanical strength [7] etc., the use of monolayer MoS_2 can be appealing in many applications in the field of spintronics and flexible electronics [8].

Now, the materials used for such high performance devices require to have higher values of thermal conductivity (κ), so that the excess heat generated can efficiently be spread out [9]. But, due to the low group velocities of acoustic phonons and extremely short intrinsic phonon mean free path, the κ of monolayer MoS_2 is significantly lower than that of single layer graphene [10,11]. However, its application as a 2D thermoelectric material is very promising, as the TE FOM (thermoelectric figure of merit) can be improved largely, by tuning the κ value, [11,12] along with a very high Seebeck coefficient (which is already reported in [13]).

So far, the various electrical properties of the monolayer and the few-layer MoS_2 had been studied extensively [1,14–19]. On the contrary, a very few had been reported until now, to describe their thermal behaviour [8–11,20,21]. In [11], the phonon thermal conductivity of monolayer MoS_2 sheet (obtained from the molecular dynamics simulations) had been found as 1.35 W m^{-1} K^{-1}, whereas in [9], using ab initio calculations, Li et al. had reported a

* Corresponding author.
E-mail addresses: dipsah_etc@yahoo.co.in (D. Saha), santanu@dese.iisc.ernet.in (S. Mahapatra).

http://dx.doi.org/10.1016/j.physe.2016.01.013
1386-9477/

κ value of 83 W m^{-1} K^{-1} at room temperature. Li et al. further demonstrated, a 30% enhancement in κ, with the increase in sample size from 1 μm to 10 μm. However, their results were obtained for the samples with complete rough edges. [9]. Besides, in [20], we find a κ value ~23.2 W m^{-1} K^{-1} at RT, which had been calculated using the combination of density functional perturbation theory (DFPT) and non-equilibrium Green's functions (NEGF) approach. Cai et al. had manifested that for monolayer MoS_2, the Grüneissen parameter values for all the modes (whether, it is acoustic, or optical) are always positive. But, their study does not include any consideration of extrinsic scattering mechanism, such as, phonon-boundary scattering which plays a critical role in precisely determining the thermal conductivity at low temperatures [20]. Apart from those theoretical calculations, we also find a measured value of κ ~34.5 W m^{-1} K^{-1}, for a suspended monolayer MoS_2 flake as reported in [10].

Owing to this large variance in the results, so far reported in literature, here we are motivated to present a comprehensive study on the lattice thermal conductivity of the monolayer MoS_2. Moreover, with the increasing use of TMDs in various fields of nanoelectronics, it becomes essential to develop an analytical model of κ which will not only impart quick estimation of heat transfer, but also be useful to know the thermal stability of the material. In the following, we first develop the closed-form expressions for the specific heat of various acoustic modes, under the approximations of Debye model. Subsequently, we derive the mode dependent lattice thermal conductivities of monolayer MoS_2 with the help of those closed-form expressions. Such an analytical approach for finding the κ can also be very useful to set insight into the electro-thermal behaviour of the two dimensional TMDs (in this case, monolayer MoS_2) through any standard CAD tool. Our result shows the value of κ as 34.06 W m^{-1} K^{-1} at RT, which is in close agreement with the experimental finding of [10], as well the other numerical results.

2. Methodology

In this study, the first-principles calculations are carried out using ATK (Atomistix Tool Kit) DFT with the local density approximation (LDA) exchange correlation (along with Perdew and Wang functional) and double zeta polarized basis set. For the hexagonal unit cell, the lattice constant is opted as 3.16 Å which is consistent with the measured value as reported in [22]. Along the *c*-axis, a vacuum region greater than 16 Å has been maintained to avoid the interactions that arise while calculating the periodic boundary conditions [9,20]. The phonon dispersion curves for the unit cell of MoS_2 are obtained using frozen phonon calculations which requires the formation of a dynamical matrix of the system. To construct the dynamical matrix, the system is automatically repeated to create a larger cell (in this work $9 \times 9 \times 1$), which is controlled by a repeat parameter [23]. Besides, the density mesh cut off is set to 75 Hartree. The phonon band structure of the monolayer MoS_2 obtained from the ab initio calculations is shown in Fig. 1.

In [10], Yan et al. reported the temperature dependent Raman spectra of the suspended monolayer MoS_2 for various cryostat temperature values ranging from 100 K to 320 K. Furthermore, they observed two sharp peaks ~385 and 405 cm^{-1} which correspond to the E^1_2g mode and the A_1g mode (denoting the in-plane and the out-of-plane vibrations) [5,10]. Since the phonon group velocities of the acoustic modes are significantly higher than those of the optical modes, thereby while determining thermal conductivity of the monolayer MoS_2, we have considered only the three acoustic modes, which are two in-plane (longitudinal acoustic (LA) and transverse acoustic (TA)) modes and one out-of-plane acoustic mode (ZA mode). Besides, as illustrated in [20], the values of the Grüneissen parameters for the LA, TA, and ZA modes are much larger than those of the optical modes, suggesting the weaker anharmonicity of the optical modes.

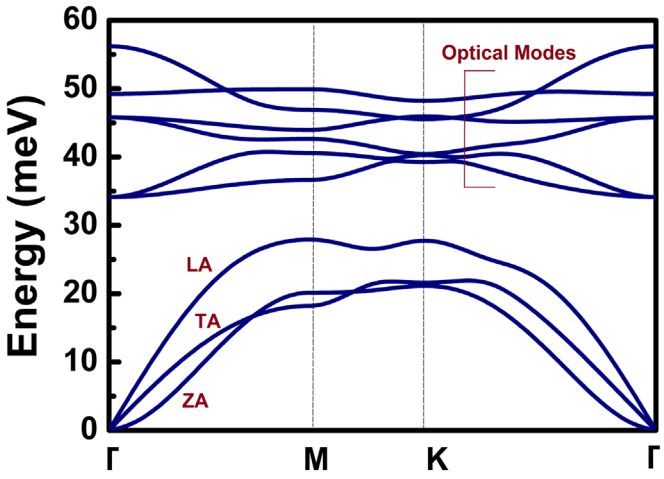

Fig. 1. Phonon dispersion curves (acoustic as well as optical modes) for the monolayer MoS_2.

3. Calculations of lattice thermal conductivity of the monolayer MoS_2

Thermal conductivity, one of the basic properties of any material relating to the thermal transport, depends strongly on the temperature whenever we opt for a wide range of temperature variation. Now, considering the in-plane κ to be isotropic for monolayer MoS_2 [9,11], we can write [10,24]

$$\kappa = \frac{1}{A\delta}\sum_{\lambda}\int_0^{q_{max}} C_{ph,\lambda}(v_\lambda)^2\tau_{eff,\lambda}\, dq, \tag{1}$$

where κ represents the thermal conductivity due to the lattice vibration taking into account the contributions from various acoustic modes (λ). δ is the thickness of the monolayer MoS_2, q is the magnitude of the wave vector, A is the molar area of the unit cell of MoS_2 with a lattice constant of a=3.16 Å. Moreover, $C_{ph,\lambda}$, v_λ, and $\tau_{eff,\lambda}$ denote the mode dependent values of specific heat, phonon group velocity and effective scattering respectively. Besides, it is worth a mention here that the intrinsic κ of the monolayer of MoS_2 is actually dominated by the phonons (because the charge carriers contribute significantly less) [20].

3.1. Closed-form analytical expressions of the mode dependent C_{ph}

In this subsection, we will try to estimate the lattice heat capacity of the monolayer suspended MoS_2, which comes mainly from the contribution of phonons [25,26]. Specific heat, which shows how the internal energy (U) of the vibrating crystal varies with temperature (T) change, can be defined at constant volume or at constant pressure [27]. Under the approximations of Debye model, the internal energy of the system can be defined as $U(T) = \int_0^{\omega max} \frac{\hbar\omega}{\left(\exp\left(\frac{\hbar\omega}{k_BT}\right)-1\right)} \times \rho(\omega)\, d\omega$, where $\rho(\omega)$ is the phonon density of states (DOS), ω_{max} is the upper cut-off frequency relating to highest phonon energy and $\frac{1}{\left(\exp\left(\frac{\hbar\omega}{k_BT}\right)-1\right)}$ denotes the Bose–Einstein distribution function [26–28]. Besides, $\hbar$ is the reduced Planck constant and k_B is the Boltzmann constant. Now, taking the

volumetric heat capacity ($\frac{\partial U}{\partial T}$) into account, we can express the specific heat contributed by the modes ($\lambda \sim$ LA, TA as [25,27]

$$C_{ph_{LA,TA}} = \frac{A\hbar^2}{2\pi\langle v_\lambda\rangle^2 k_B T^2}\int_0^{\omega max,\lambda} \omega_\lambda^3 \times \frac{\exp\left(\frac{\hbar\omega_\lambda}{k_B T}\right)}{\left(\exp\left(\frac{\hbar\omega_\lambda}{k_B T}\right)-1\right)^2} d\omega_\lambda. \quad (2)$$

where the 2D phonon density of states for the LA and TA modes had been replaced by $\rho(\omega_\lambda) = \frac{A}{(2\pi)^2} \times 2\pi q\left[\frac{1}{d\omega_\lambda / dq}\right] = \frac{A\omega_\lambda}{(2\pi)\langle v_\lambda\rangle^2}$, with help of the linear approximation of the dispersion relation, that is, $\omega_\lambda(q) = \langle v_\lambda\rangle q$. Besides, $\langle v_\lambda\rangle$ is the mode specific average group velocity. However, for the out-of-plane acoustic mode ($\lambda \sim$ZA), the dispersion relation is obtained as $\omega_\lambda(q) = \alpha_d q^2$, where the α_d can actually be fitted from the phonon dispersion curve of ZA branch (as shown in Fig. 1). Thereby, the phonon density of states for the ZA mode becomes $\rho(\omega_\lambda) = \frac{A}{(4\pi)\alpha_d}$, and the specific heat contributed by ZA mode is calculated as [25,27]

$$C_{ph_{ZA}} = k_B \int_0^{\omega max,\lambda} \frac{\hbar^2\omega_\lambda^2}{k_B^2 T^2} \times \left(\frac{A}{4\pi\alpha_d}\right) \frac{\exp\left(\frac{\hbar\omega_\lambda}{k_B T}\right)}{\left(\exp\left(\frac{\hbar\omega_\lambda}{k_B T}\right)-1\right)^2} d\omega_\lambda. \quad (3)$$

The Debye temperature used for finding the enthalpy and heat capacity of bulk MoS_2, can be found as 300 K, as reported in [29]. But such a value of Debye temperature, which is obtained from the low temperature specific heat, may not be accurate, if we only consider the acoustic modes [30]. For the monolayer of MoS_2, we derived the mode dependent Debye temperature with help of the upper cut-off frequencies for various acoustic modes, and it may be expressed as $T_{D,\lambda} = 2\sqrt{\pi}\frac{\hbar}{k_B}\left\langle v_\lambda\right\rangle\sqrt{\frac{N_\lambda}{A}}$, where the upper cut-off frequencies for the LA, TA and ZA modes are related to the total number of vibrating states (N_λ) as $\omega_{max,\lambda} = \sqrt{4\pi\langle v_\lambda\rangle^2 (N_\lambda/A)}$. Moreover, with information of phonon DOS, N_λ can be obtained using the relation $N_\lambda = \int_0^{\omega max,\lambda} \rho(\omega_\lambda)\, d\omega_\lambda$. Hence, the total lattice heat capacity of the monolayer suspended MoS_2, considering the contributions from the individual modes, can be found as $C_{ph} = (C_{ph_{LA}} + C_{ph_{TA}} + C_{ph_{ZA}})$ [28,31]. The upper cut-off frequency values used for the specific heat calculation of different modes are taken as 4.08×10^{13} Hz, 3.15×10^{13} Hz, and 3.29×10^{13} Hz, whereas the average group velocity values are found to be 1325 m/s, 915 m/s, and 972 m/s for LA, TA and ZA modes respectively. However, the analytical solutions of (2) and (3) are available at the two extreme limits, that is, for $T \gg T_{D,\lambda}$ and $T \ll T_{D,\lambda}$ [26,32]. Under the approximations of the Debye model, with the linear and isotropic phonon dispersion, C_{ph} will approach a constant value at higher temperatures (denoted by the classical Dulong–Petit limit in case of 3D crystals), whereas at low temperatures it shows a $\sim T^3$ dependency for bulk and generally a $\sim T^n$ dependency (where $1 \le n \le 2$) for 2D crystals [31,32]. But, here in this work, our aim is to study the thermal behaviour of the monolayer MoS_2 in the low-to-intermediate range of temperature values which lie $\pm$250 K around the room temperature (300 K). In order to do so, we have derived the following closed-form expressions (as illustrated in (4) and (5)), which work fine for the entire temperature range of 30–550 K:

$$C_{ph_{LA,TA}} = 2\pi \times k_B A \times \left(\frac{k_B T}{h\langle v_{LA,TA}\rangle}\right)^2 \times \left(\frac{f1}{2.4 \times \pi \times 10}\right), \quad (4)$$

where h denotes the Planck constant, besides $f1 = x_{d_{LA,TA}}^3\left[\frac{1}{\left(1-\exp\left(x_{d_{LA,TA}}\right)\right)} - 2.4\right] + 3x_{d_{LA,TA}}^2 \times (C1 - C2) - \left(3x_{d_{LA,TA}} \times \ln(\exp(2.5x_{d_{LA,TA}}) - 1)\right)$, and $x_{d_{LA,TA}} = \left(\frac{\hbar \times \omega max_{LA,TA}}{k_B T}\right)$. $C1$ and $C2$ are used as model parameters (calibrated against the numerical results) with the values 4.6π and 0.05 for the LA mode and 3.8π and 0.05 for the TA mode. For, the ZA mode with $\alpha_d = 2.11 \times 10^{-7}$, we have found

$$C_{ph_{ZA}} = -4.5 \times 10^{-15}\left(\frac{\hbar^2\omega_{max,ZA}^3}{3.5k_B^2T^2}\right) - 3 \times 10^{-15} \times \left(\frac{\hbar\omega_{max,ZA}^2}{3.5k_B T}\right) + 4.5\pi \times 1 \times 10^{-14}(\omega_{max,ZA}). \quad (5)$$

As shown in Fig. 2(a), considering the temperature variations from 30 K to 550 K, the C_{ph} calculated using (4) and (5), is closely matching with the value of that obtained by summing the numerical solutions of (2) and (3). Fig. 2(b) shows the relative contributions of the LA, TA and ZA modes to the total heat capacity. We find, at RT, both the LA and the TA modes contribute almost equally to the total C_{ph}, whereas the relative contribution of the ZA mode is significantly less ($\sim$50% of the individual LA or TA mode). However, owing to the combined effect of the individual modes, we observe that the total lattice heat capacity of the monolayer MoS_2 shows a $T^{1.1}$ dependency at low temperatures ($C_{ph} \propto T^{1.1}$, $\sim$ 50 K or below).

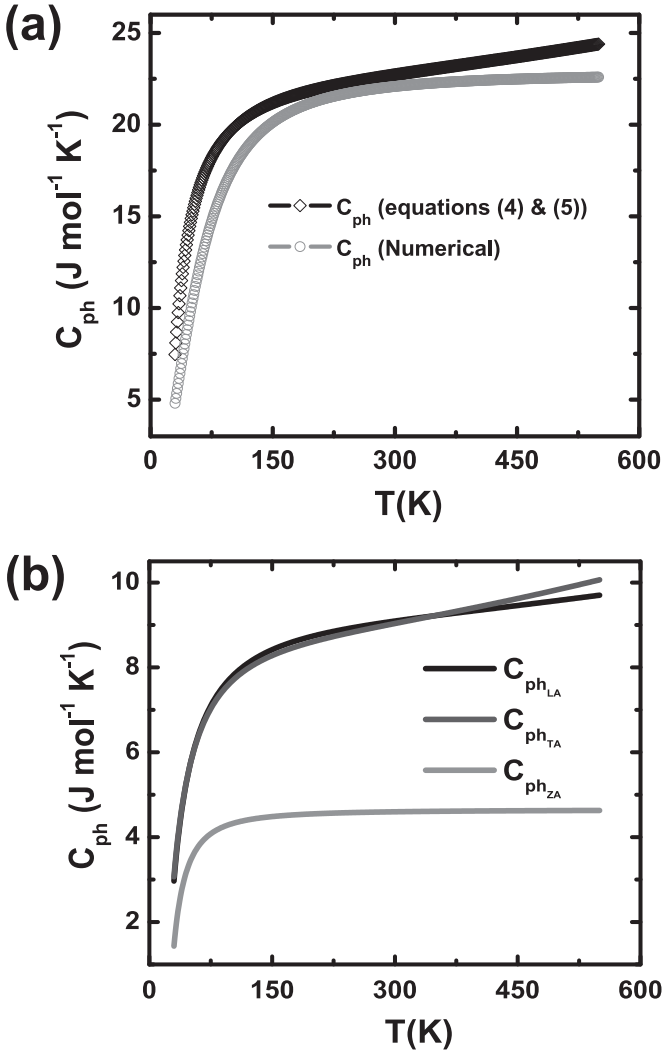

Fig. 2. (a) Temperature dependence of the total phonon specific heat of monolayer MoS_2. (b) Mode specific contributions of the three acoustic modes to the C_{ph} (calculated using (4) and (5)).

3.2. Mode specific group velocities, $v_\lambda(q)$

Although, while calculating C_{ph} under the approximations of Debye model, we have taken a linear dispersion relation for LA and TA modes, and a quadratic dispersion relation for the ZA mode, but looking into the exact phonon dispersion relations (derived from the first-principles calculations), we can see that neither the in-plane acoustic modes are perfectly linear in between the $\Gamma - M$ points of the Brillouin Zone (BZ), nor the out-of-plane is truly quadratic. Therefore, for more accurate results, we utilized the following semiempirical relations which reproduce the $\omega_\lambda(q)$ (in 'Hz') for the three acoustic modes, as well as determine the mode specific group velocities $v_\lambda(q)$.

$$\omega_{LA} = \frac{e}{\hbar}\left(- 110q^2 + 110q - 0.059\right) \times 10^{-3}, \tag{6}$$

$$\omega_{TA} = \frac{e}{\hbar}\left(- 66q^2 + 71q - 0.44\right) \times 10^{-3}, \tag{7}$$

$$\omega_{ZA} = \frac{e}{\hbar}\left(- 330q^3 + 240q^2 + 3.7q - 0.054\right) \times 10^{-3}, \tag{8}$$

where e denotes the charge of an electron. Fig. 3(a) shows the variation of $\omega_\lambda(q)$, whereas Fig. 3(b) illustrates the corresponding change in $v_\lambda(q)$ along the Γ–M direction of the BZ. It can be seen that the maximum velocities for the LA and TA modes are 2650 m/s and 1710 m/s respectively, near the Γ point and those reduces monotonically as we route towards the M point of BZ. For the ZA mode, the group velocity is maximum (1490 m/s) around the mid of the BZ.

Thus, with help of Eqs. (6)–(8) which are reproducing the $\omega_\lambda(q)$, $v_\lambda(q)$ analytically, and the closed-form C_{ph} as formulated earlier, we can compute (1), to obtain the phonon thermal conductivities for the LA, TA and ZA modes. Now, for the purpose of the calculation of κ we have determined the $\tau_{eff,\lambda}$ following the approach as described in the next subsection.

3.3. Phonon scatterings

To determine the $\tau_{eff,\lambda}$, we start with the consideration of an ideal crystal without having any crystal imperfections due to defects, impurities, etc. In such case, the phonon mean free path will mostly be limited by phonon–phonon scattering [25,33]. Out of the two phonon–phonon scattering processes, the Normal processes conserve the total crystal momentum as well as follow the energy conservation law. On the other hand, for the Umklapp processes of phonon–phonon scattering the crystal momentum is not conserved [33]. It is generally presumed that the momentum-conserving Normal processes play no significant and direct role in determining the thermal conductivity, whereas at room temperature and above, the Umklapp scattering plays the dominant role in finding out the thermal conductivity of the crystalline solid.

Now, a thermal conductivity determined by taking the anharmonic phonon scatterings into account can be treated as the intrinsic thermal conductivity. According to the theory described by Klemens [34], for any 2D layer, taking only basal plane phonon propagation into account, the mode dependent relaxation time due to anharmonic scattering (which is essentially considering the Umklapp processes) can be found from the relation [21,34]:

$$\tau_{anh,\lambda} \simeq \tau_{ump,\lambda} = \frac{M' v_\lambda^2 \times T_{D,\lambda}}{\hbar\left(\gamma_\lambda^2\right) \times T \times \omega_\lambda^2}, \tag{9}$$

where M' is the mass of the unit cell of MoS_2 and γ_λ represents the

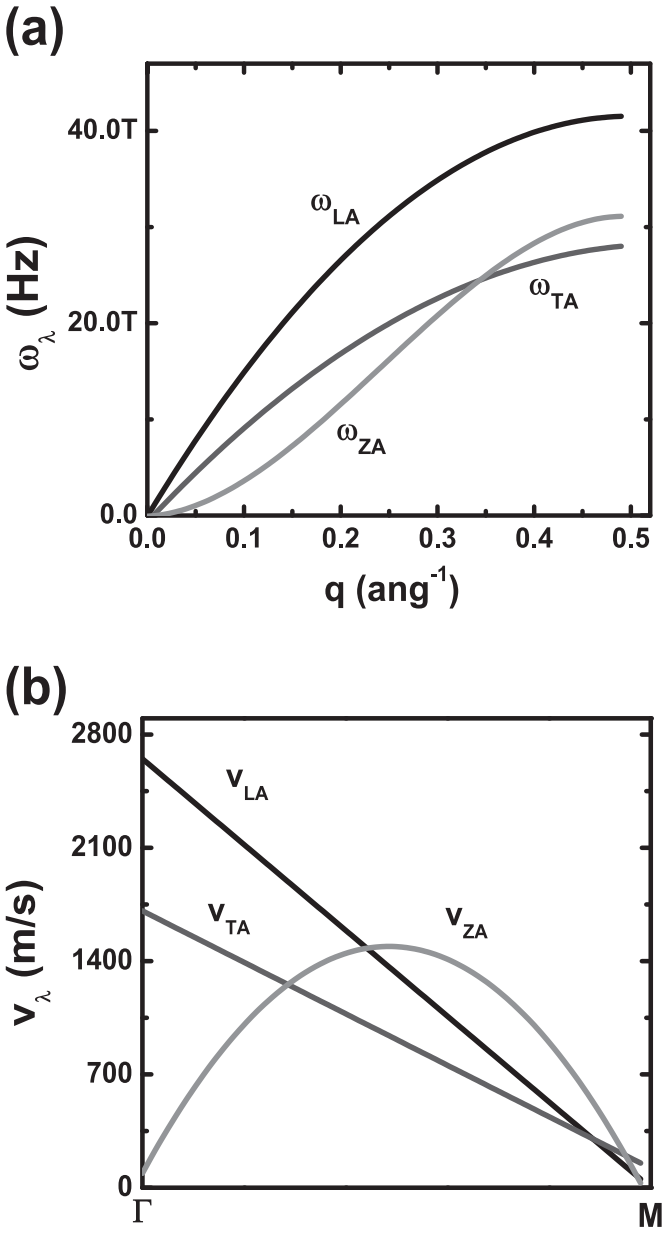

Fig. 3. (a) Variation of ω_λ with q as obtained from (6)–(8). (b) Mode specific $v_\lambda(q)$ of the acoustic modes within the Γ–M points of the BZ.

mode dependent Grüneissen parameter values. For a 2D material like MoS_2, the acoustic and the optical mode Grüneissen parameter values can be found from the plots of '*Fig. 3 (a) and (b)*' as illustrated in [20]. Near the Γ point, the Grüneissen parameter values of LA, TA and ZA modes are obtained as 25.3, 58.6, and 159.7 respectively. However, as we route towards the M point of BZ, those values get substantially reduced (~1.018 for the LA mode and ~2.00 for the TA and ZA modes).

Moreover, the $\tau_{anh,\lambda}$, which is calculated from (9), can therefore be utilized to find out the intrinsic phonon mean free path (Λ_{int}) of monolayer MoS_2 ($\Lambda_{int} = v_\lambda \times \tau_{anh,\lambda}$). In comparison with the single layer graphene, Λ_{int} of monolayer MoS_2 is much smaller. Considering the entire variation of Λ_{int} along the Γ–M direction of the BZ, we find that the Λ_{int} is ~ 17.2 nm near the Γ point for the LA mode, whereas that for the TA and ZA modes are ~ 8.32 nm and ~ 1.82 nm respectively. Apart from that as the monolayer MoS_2 sheet considered in this study is of the dimensions, L=1 μm and W=1 μm, thereby we expect the thermal transport inside the

sample to be diffusive. At low temperatures, the phonon-boundary scattering which is an extrinsic scattering mechanism, mostly affects the thermal conductivity. It is very critical to precisely determine the effect of boundary scattering, specially for small-structures where κ starts depending upon the physical dimensions of the device [25]. Taking into consideration the heat flow parallel to the MoS_2 sheet, we can determine the phonon-boundary scattering as [9,34]

$$\frac{1}{\tau_{B,\lambda}} = \frac{v_\lambda}{L} \times \left(\frac{1-p}{1+p}\right), \tag{10}$$

where the amount of diffuse phonon scattering from the edges is determined using a specularity parameter (p) that can take any value in between 0 and 1 (for a completely rough edge, $p \rightarrow 0$, for the extremely smooth edge, $p \rightarrow 1$) [9,34]. As reported in [21,35], the specularity parameter can be expressed as, $p(q) = \exp(-4 \times q^2 \times \varsigma^2)$, where the parameter ς includes information regarding the root-mean-square height of the surface roughness, as well as the angle of incident phonon at any particular point on the rough edge [35].

Moreover, to incorporate the effects of crystal imperfections, such as defects occur during the fabrication of the suspended monolayer, PMMA residues, or oxidation of the MoS_2 sample, one should take the defect scattering into account while determining the $\tau_{eff,\lambda}$. However, such a study is due for the monolayer MoS_2, as that requires further experimental evidences of thermal conductivity measurement. Hence, considering the intrinsic as well as the phonon-boundary scattering phenomenon, we can calculate the $\tau_{eff,\lambda}$ (with help of the Matthiessen's rule) as,

$$\frac{1}{\tau_{eff,\lambda}} = \frac{1}{\tau_{anh,\lambda}} + \frac{1}{\tau_{B,\lambda}}. \tag{11}$$

4. Results and discussions

In [8], Jo et al. estimated the value of p within the range of 0.3–0.6 for a few layer sample. However, here in this work, for the monolayer suspended MoS_2 sample (having, dimensions $L=1$ μm and $W=1$ μm), we have set the p value as 0.4. Besides, from the details as illustrated in Fig. 4(a) and (b), we find that how κ varies with the change in dimensions, as well as p (at RT). At $T=300$ K, we find that the impact of edge roughness becomes more severe as we lower the dimension (in this case, L) of the sample below ~ 50 nm. For all such cases (Fig. 4(a)), the phonon-boundary scattering mean free path actually becomes comparable with the physical dimensions of the MoS_2 sheet.

Next, considering the κ model as depicted earlier (with the upper cut-off frequency values for the LA, TA, and ZA modes as 4.08×10^{13} Hz, 3.15×10^{13} Hz, and 3.29×10^{13} Hz respectively, and $\delta = 6.033 \times 10^{-10}$ m), we have plotted the variation of thermal conductivity with the change in T (Fig. 5). To validate the lattice thermal conductivity value as computed here, we consider the experimental results of [10], where the suspended monolayer MoS_2 flake (which is placed on the $Si_3N_4/SiO_2/Si$ perforated grid like substrate) of diameter 1.2 μm, obtains a κ value of 34.5 ± 4 $W\,m^{-1}\,K^{-1}$ at RT.

Now, as shown in Fig. 5, the κ of the suspended monolayer MoS_2 obtained using the model described in this work, closely matches with the measured result of [10] as well as the other theoretical calculations [21]. At RT, κ is calculated as 34.06 $W\,m^{-1}\,K^{-1}$, in which the relative contributions of the LA, TA and ZA modes are ~63%, ~17%, and ~20% respectively. However, for a low temperature, such as, 40 K, the relative contribution of the LA mode reduces to ~48%, whereas the contribution of the ZA mode increases to ~32%. Besides, it is important to notice that the effect of the anharmonic scattering becomes dominant in determining the κ, as we increase the temperature beyond 60 K.

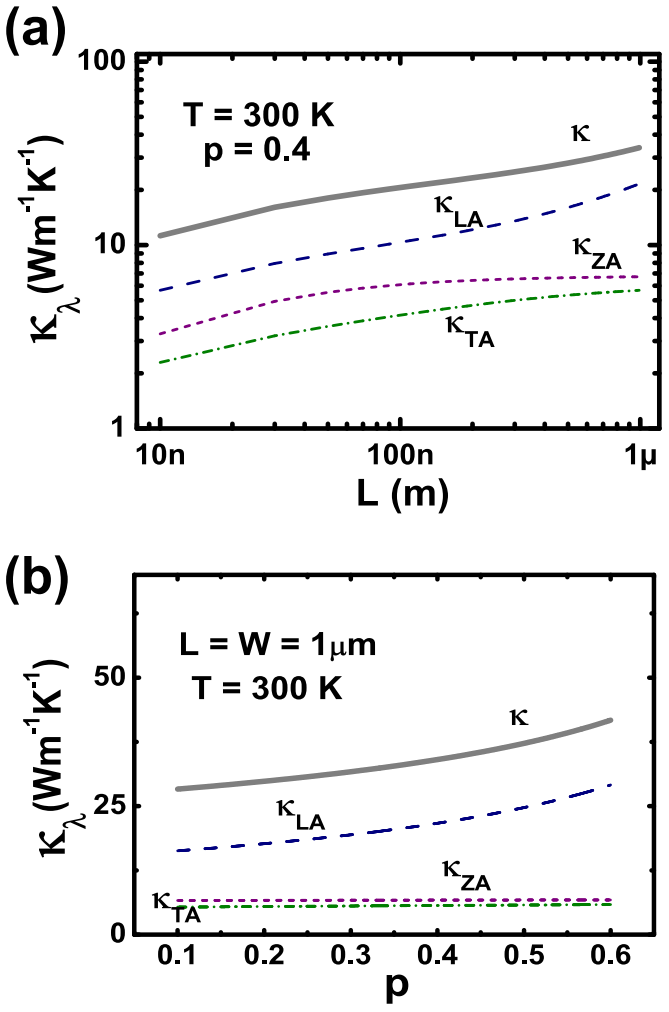

Fig. 4. (a) Variation of thermal conductivity with the change in L. (b) p dependency of κ_λ at RT for a sample with dimensions $L=W=1$ μm.

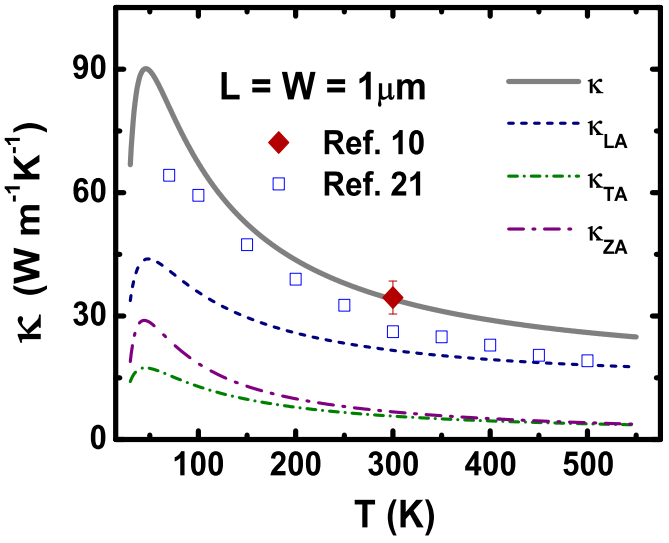

Fig. 5. Calculated thermal conductivity of the monolayer MoS_2 (represented by the solid line), along with the relative contributions of LA, TA and ZA modes (dotted lines).

5. Conclusion

In conclusion, we have presented a comprehensive study on the phonon thermal conductivity of a suspended monolayer MoS_2, with the very basic objective of finding an analytical approach for determining the κ. For the purpose, we have developed closed-form expressions of the mode specific heat capacities, as well as derived the analytical solutions of mode dependent group velocities. Later, with help of those analytic expressions, we have computed the phonon thermal conductivities of the monolayer MoS_2 which works for the entire temperature range of 30–550 K. Besides modelling the intrinsic κ, we have also analysed the effects of edge roughness on thermal conductivity. Considering the relative contributions of LA, TA and ZA modes, the κ of the monolayer MoS_2 has been calculated as 34.06 $W\,m^{-1}\,K^{-1}$ (at room temperature), which shows a good agreement with the experimental result.

Acknowledgement

Authors would like to thank Dr. Anders Blom and Dr. Umberto Martinez Pozzoni of QuantumWise A/S Copenhagen, Denmark, for the useful discussions.

References

[1] B. Radisavljevic, A. Radenovic, J. Brivio, V. Giacometti, A. Kis, Single-layer MoS_2 transistors, Nat. Nanotechnol. 6 (2011) 147–150.
[2] P. Miró, M. Audiffred, T. Heine, An atlas of two-dimensional materials, Chem. Soc. Rev. 43 (2014) 6537–6554.
[3] L. Lin, Y. Xu, S. Zhang, I.M. Ross, A.C.M. Ong, D.A. Allwood, Fabrication of luminescent monolayered tungsten dichalcogenides quantum dots with giant spin-valley coupling, ACS Nano 7 (2013) 8214–8223.
[4] K.F. Mak, C. Lee, J. Hone, J. Shan, T.F. Heinz, Atomically thin MoS_2: a new direct-gap semiconductor, Phys. Rev. Lett. 105 (2010) 136805.
[5] C. Lee, H. Yan, L.E. Brus, T.F. Heinz, J. Hone, S. Ryu, Anomalous lattice vibrations of single- and few-layer MoS_2, ACS Nano 4 (5) (2010) 2695–2700.
[6] D. Xiao, G.-B. Liu, W. Feng, X. Xu, W. Yao, Coupled spin and valley physics in monolayers of MoS_2 and other group-VI dichalcogenides, Phys. Rev. Lett. 108 (2012) 196802.
[7] S. Bertolazzi, J. Brivio, A. Kis, Stretching and breaking of ultrathin MoS_2, ACS Nano 5 (12) (2011) 9703–9709.
[8] I. Jo, M.T. Pettes, E. Ou, W. Wu, L. Shi, Basal-plane thermal conductivity of few-layer molybdenum disulfide, Appl. Phys. Lett. 104 (2014) 201902.
[9] W. Li, J. Carrete, N. Mingo, Thermal conductivity and phonon linewidths of monolayer MoS_2 from first principles, Appl. Phys. Lett. 103 (2013) 253103.
[10] R. Yan, J.R. Simpson, S. Bertolazzi, J. Brivio, M. Watson, X. Wu, A. Kis, T. Luo, A. R. Hight Walker, H.G. Xing, Thermal conductivity of monolayer molybdenum disulfide obtained from temperature-dependent Raman spectroscopy, ACS Nano 8 (1) (2014) 986–993.
[11] X. Liu, G. Zhang, Q.-X. Pei, Y.-W. Zhang, Phonon thermal conductivity of monolayer MoS_2 sheet and nanoribbons, Appl. Phys. Lett. 103 (2013) 133113.
[12] R. Verma, S. Bhattacharya, S. Mahapatra, Thermoelectric performance of a single-layer graphene sheet for energy harvesting, IEEE Trans. Electron. Devices 60 (6) (2013) 2064–2070.
[13] M. Buscema, et al., Large and tunable photothermoelectric effect in single-layer MoS_2, Nano Lett. 13 (2013) 358–363.
[14] D. Lembke, A. Kis, Breakdown of high-performance monolayer MoS_2 transistors, ACS Nano 6 (11) (2012) 10070–10075.
[15] S. Das, H.-Y. Chen, A.V. Penumatcha, J. Appenzeller, High performance multilayer MoS_2 transistors with scandium contacts, ACS Nano Lett. vol. 13 (2013) 100–105.
[16] M. Ghorbani-Asl, S. Borini, A. Kuc, T. Heine, Strain-dependent modulation of conductivity in single-layer transition-metal dichalcogenides, Phys. Rev. B 87 (2013) 235434.
[17] H. Schmidt, et al., Transport properties of monolayer MoS_2 grown by chemical vapor deposition, Nano Lett. 14 (2014) 1909–1913.
[18] C.D. English, G. Shine, V.E. Dorgan, K.C. Saraswat, E. Pop, Improving contact resistance in MoS_2 field effect transistors, in: 72nd Annual Device Research Conference, 2014, pp. 193–194.
[19] R. Ganatra, Q. Zhang, Few-layer: MoS_2: A promising layered semiconductor, ACS Nano 8 (5) (2014) 4074–4099.
[20] Y. Cai, J. Lan, G. Zhang, Y.-W. Zhang, Lattice vibrational modes and phonon thermal conductivity of monolayer MoS_2, Phys. Rev. B 89 (2014) 035438.
[21] X. Wei, Y. Wang, Y. Shen, G. Xie, H. Xiao, J. Zhong, G. Zhang, Phonon thermal conductivity of monolayer: MoS_2: A comparison with single layer graphene, Appl. Phys. Lett. 105 (2014) 103902.
[22] T. Böker, R. Severin, A. Müller, C. Janowitz, R. Manzke, D. Voss, P. Krüger, A. Mazur, J. Pollmann, Band structure of MoS_2, $MoSe_2$, and α- $MoTe_2$: Angle-resolved photoelectron spectroscopy and ab initio calculations, Phys. Rev. B 64 (2001) 235305.
[23] Phonons: Bandstructure, thermal transport, thermo-electrics, Tutorial: Atomistix ToolKit (Version 2014.0) ⟨http://www.quantumwise.com⟩.
[24] M.G. Holland, Analysis of lattice thermal conductivity, Phys. Rev. 132 (6) (1963) 2461–2471.
[25] D.L. Nika, A.A. Balandin, Two-dimensional phonon transport in graphene, J. Phys.: Condens. Matter 24 (2012) 233203.
[26] J. Hone, Phonons and thermal properties of carbon nanotubes, Top. Appl. Phys. 80 (2001) 273–286.
[27] C. Kittel, Introduction to Solid State Physics, 7th ed., NA John Wiley & Sons (ASIA) Pte. Ltd., Singapore.
[28] A. Alofi, G.P. Srivastava, Phonon conductivity in graphene, J. Appl. Phys. 112 (2012) 013517.
[29] L.S. Volovik, et al., Enthalpy and heat capacity of molybdenum disulfide, Sov. Powder Metallurgy and Metal Ceramics 17 (9) (1978) 697–702.
[30] D.T. Morelli, J.P. Heremans, Estimation of the isotope effect on the lattice thermal conductivity of group IV and group III–V semiconductors, Phys. Rev. B 66 (2002) 195304.
[31] D.L. Nika, A.I. Cocemasov, A.A. Balandin, Specific heat of twisted bilayer graphene: engineering phonons by atomic plane rotations, Appl. Phys. Lett. 105 (2014) 031904.
[32] R. Pässler, Dispersion-related theory for heat capacities of semiconductors, Phys. Status Solidi B 244 (12) (2007) 4605–4623.
[33] J. Callaway, Model for lattice thermal conductivity at low temperatures, Phys. Rev. 113 (4) (1959) 1046–1051.
[34] P.G. Klemens, Theory of thermal conduction in thin ceramic films, Int. J. of Thermophys. 22 (1) (2001) 265–275.
[35] Z. Aksamija, I. Knezevic, Lattice thermal transport in large-area polycrystalline graphene, Phys. Rev. B 90 (2014) 035419.